PLOS ONE

RESEARCH ARTICLE

Intronic miR-6741-3p targets the oncogene *SRSF3*: Implications for oral squamous cell carcinoma pathogenesis

Dhanashree Anil More[1], Nivedita Singh[1], Radha Mishra[1], Harsha Pulakkat Muralidharan[1], Kodaganur Srinivas Gopinath[2], Champaka Gopal[3], Arun Kumar[1]*

1 Department of Developmental Biology and Genetics, Indian Institute of Science, Bengaluru, India, **2** Department of Surgical Oncology, HCG-Bangalore Institute of Oncology, Bengaluru, India, **3** Department of Pathology, Kidwai Memorial Institute of Oncology, Bengaluru, India

* arunk@iisc.ac.in

Citation: More DA, Singh N, Mishra R, Muralidharan HP, Gopinath KS, Gopal C, et al. (2024) Intronic miR-6741-3p targets the oncogene *SRSF3*: Implications for oral squamous cell carcinoma pathogenesis. PLoS ONE 19(5): e0296565. https://doi.org/10.1371/journal.pone.0296565

Editor: Younghoon Kee, Daegu-Gyeongbuk Institute of Science & Technology Graduate School, REPUBLIC OF KOREA

Received: December 28, 2023

Accepted: April 23, 2024

Published: May 23, 2024

Data Availability Statement: All relevant data are within the manuscript and its Supporting information file.

Funding: This work was funded by a grant (# BT/PR33054/MED/30/2210/2020) from the Department of Biotechnology, New Delhi.

Competing interests: The authors have declared that no competing interests exist.

Abstract

Epigenetic silencing through methylation is one of the major mechanisms for downregulation of tumor suppressor miRNAs in various malignancies. The aim of this study was to identify novel tumor suppressor miRNAs which are silenced by DNA hypermethylation and investigate the role of at least one of these in oral squamous cell carcinoma (OSCC) pathogenesis. We treated cells from an OSCC cell line SCC131 with 5-Azacytidine, a DNA methyltransferase inhibitor, to reactivate tumor suppressor miRNA genes silenced/downregulated due to DNA methylation. At 5-day post-treatment, total RNA was isolated from the 5-Azacytidine and vehicle control-treated cells. The expression of 2,459 mature miRNAs was analysed between 5-Azacytidine and control-treated OSCC cells by the microRNA microarray analysis. Of the 50 miRNAs which were found to be upregulated following 5-Azacytidine treatment, we decided to work with miR-6741-3p in details for further analysis, as it showed a mean fold expression of >4.0. The results of qRT-PCR, Western blotting, and dual-luciferase reporter assay indicated that miR-6741-3p directly targets the oncogene *SRSF3* at the translational level only. The tumor-suppressive role of miR-6741-3p was established by various *in vitro* assays and *in vivo* study in NU/J athymic nude mice. Our results revealed that miR-6741-3p plays a tumor-suppressive role in OSCC pathogenesis, in part, by directly regulating *SRSF3*. Based on our observations, we propose that miR-6741-3p may serve as a potential biological target in tumor diagnostics, prognostic evaluation, and treatment of OSCC and perhaps other malignancies.

Introduction

Oral squamous cell carcinoma (OSCC), arising from surface epithelium, accounts for more than 90% of all oral malignancies [1]. Tumors arising in the oral and oropharyngeal mucosa, including those of the tongue and lips collectively represent the 16th most common cancer worldwide with an annual incidence of 377,713 new cases and 177,757 deaths [2, 3]. In India,

oral cancer is the most common cancer in males and the fourth most common cancer in females with an ASR (age-standardized rate) of 14.8 and 4.6 per 100,000 males and females respectively [2, 3]. Despite recent advances in cancer diagnosis and treatment, including targeted therapy against EGFR using the monoclonal antibody Cetuximab, the 5-year survival rate for oral cancer has remained less than 50% over the last 50 years [4, 5]. The current scenario, therefore, requires the identification of new therapeutic targets and molecular markers to aid in better prognosis and treatment.

In recent years, the critical role of microRNAs (miRNAs/miRs) in cancer progression has been widely acknowledged. MicroRNAs belong to a class of endogenous small non-coding RNA molecules of 20–25 nucleotides length, found mostly in eukaryotes, and regulate gene expression by inducing degradation or inhibiting translation of target mRNAs by binding to either the 3'UTRs (untranslated regions), the 5'UTRs or the coding sequences (CDSs) of their target mRNAs [6]. Apart from their specific functions in biological processes such as cell proliferation, differentiation, apoptosis, development, etc., miRNAs are dysregulated in a wide variety of diseases such as immune disorders, Alzheimer's disease, cardiovascular diseases, rheumatoid arthritis, cancer, etc. [7]. Many functional studies and clinical analysis have linked miRNA dysregulation as a causal factor for cancer progression [8]. Numerous studies have shown that microRNA-based therapeutics hold promising potential for cancer management and hence there is a growing need to further explore their roles in various cancers with the aim of developing miRNA therapeutics [7, 8].

MicroRNAs can function as oncogenes or tumor suppressor genes and drive the process of carcinogenesis. The involvement of several tumor suppressor miRNAs like miR-15a, miR-16a, let-7 family, miR-143, miR-145, and oncogenic miRNAs like miR-155, miR-17 cluster and miR-21 in several malignancies including OSCC has been established [8, 9]. Aberrant expression of tumor suppressor and oncogenic miRNAs drives the progression from oral premalignant lesions to cancer and also correlates with and could explain the pathogenesis, metastasis, and chemoresistance of OSCC [10, 11]. Of the various mechanisms reported to be involved in miRNA deregulation such as loss or mutation of miRNA-encoding genes, defective biogenesis pathway, hypermethylation-mediated silencing of miRNA-encoding genes, and/or histone modifications, epigenetic silencing through methylation of the promoter regions has emerged as the major mechanism of silencing/downregulation of tumor suppressor miRNAs [12, 13]. Also, the two major risk factors of oral cancer, namely smoking and alcohol consumption are reported to impact the epigenetic regulation of various protein-coding genes and miRNAs that are directly involved in OSCC carcinogenesis [14]. Thus, the above observations emphasize a critical role of epigenetically regulated tumor suppressor miRNAs in OSCC pathogenesis.

For the identification of epigenetically regulated miRNAs, a majority of studies employ chromatin-modifying agents or epigenetic modifiers such as DNA hypomethylation agents (DNA methyltransferase inhibitors) like 5-Azacytidine or histone deacetylase (HDAC) inhibitors like 4-phenylbutyric acid (PBA) and trichostatin A (TSA), and in most cases a combination of both to treat cells from cancer cell lines and later adopt a microarray-based approach to identify miRNAs which are differentially expressed between untreated and drug-treated cells [13, 15]. In the present study, by comparing the miRNA expression profiles of 5-Azacytidine and vehicle control-treated OSCC cells followed by the microRNA microarray analysis, we have identified a total of 50 DNA methylation silenced/downregulated miRNAs, and investigated the role of one of these, miR-6741-3p in great details.

Results

miR-6741-3p is upregulated following 5-Azacytidine treatment of SCC131 cells

In order to identify methylation silenced/downregulated tumor suppressor miRNAs, cells from an OSCC cell line SCC131 were treated separately with 5-Azacytidine and vehicle-control (DMSO). To increase sensitivity in the microRNA microarray analysis, total RNA was isolated using a mirVana™ miRNA isolation kit as it specifically enriches for small RNAs (<200 nucleotides). To ascertain the efficacy of the 5-Azacytidine treatment on SCC131 cells, the expression of a known tumor suppressor gene *MCPH1*, which is reported to be epigenetically silenced in SCC131 cells [16], was evaluated by qRT-PCR (Fig 1A). The results revealed increased expression of *MCPH1* following 5-Azacytidine treatment, indicating that the treatment of SCC131 cells with 5-Azacytidine was effective. Following this, the expression of 2,549 mature miRNAs was investigated by the microRNA microarray analysis using SurePrint G3 8x60K Human miRNA Microarray chips. Using a cut-off of 0.8-fold expression change, 50 miRNAs were found to be upregulated and 28 miRNAs were found to be downregulated after the 5-Azacytidine treatment compared to the vehicle control (Fig 1B, S1 Table). We decided to work with one of these microRNAs, miR-6741-3p for further analysis as it was found to be upregulated, showed a mean fold expression of 4.96 following the 5-Azacytidine treatment, and there is a lack of reports regarding its role in tumorigenesis (S1 Table).

The upregulation of miR-6741-3p following 5-Azacytidine treatment was validated by qRT-PCR using RT6 and short-miR specific primers (S2 Table). As expected, a significant upregulation in miR-6741-3p expression was observed in 5-Azacytidine treated cells compared to the vehicle control treated cells, thus validating the miRNA microarray data (Fig 1C).

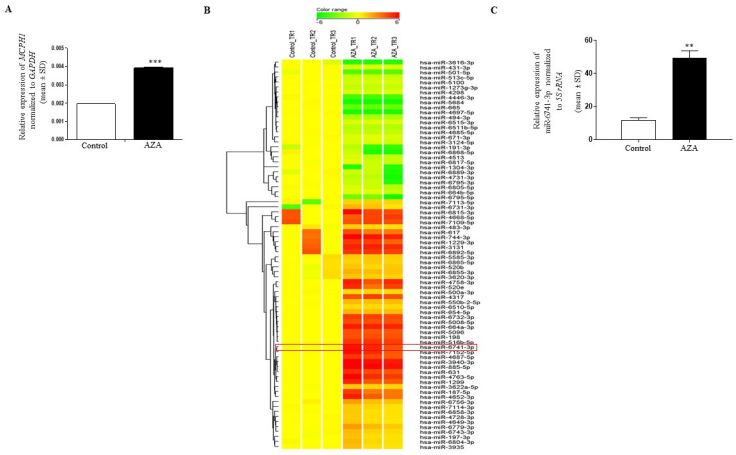

Fig 1. MicroRNA microarray analysis of 5-Azacytidine and control treated SCC131 cells. (A) The expression of the tumor suppressor gene *MCPH1* was found to be upregulated following 5-Azacytidine treatment of SCC131 cells by qRT-PCR. (B) A heatmap depicting the upregulation of 50 miRNAs and downregulation of 28 miRNAs expression following 5-Azacytidine treatment of SCC131 cells. The change in expression of miR-6741-3p is highlighted. Control_TR1, Control_TR2 and Control_TR3 represent technical replicates of RNA from DMSO treated cells. AZA_TR1, AZA_TR2 and AZA_TR3 are technical replicates of RNA from 5-Aacytidine treated cells. (C) Validation of miR-6741-3p upregulation following 5-Azacytidine treatment of SCC131 cells by qRT-PCR. Each bar for qRT-PCR is an average of 2 technical replicates. *Abbreviation*: AZA, 5-Azacytidine.

https://doi.org/10.1371/journal.pone.0296565.g001

miR-6741-3p overexpression decreases the proliferation of SCC131 and SCC084 cells

Epigenetic silencing due to DNA methylation is one of the key mechanisms for the repression of tumor suppressor miRNAs. As miR-6741-3p was found to be upregulated following 5-Aza-cytidine treatment of SCC131 cells, we hypothesized that it could be a tumor suppressor miRNA and therefore decided to ascertain its involvement in the regulation of various aspects of cancer cells. To check the involvement of miR-6741-3p in controlling cell proliferation, we transiently transfected SCC131 and SCC084 cells with pcDNA3-*EGFP* (vector control) and pmiR-6741 separately and performed the trypan blue dye exclusion assay. The results showed that miR-6741-3p decreased cell proliferation compared to the vector control in both the cell lines, thus suggesting its role as a tumor suppressor miRNA (S1 Fig).

In silico identification of gene target(s) of miR-6741-3p

Three different mRNA target prediction algorithms (e.g., TargetScan, miRDB, and DIANA microT-CDS) were used to identify gene target(s) for miR-6741-3p. We found *SRSF3* (serine/arginine-rich splicing factor 3), *C6ORF89* (chromosome 6 open reading frame 89), *NDST2* (N-deacetylase/N-sulfotransferase (heparan glucosaminyl) 2), and *MKX* (mohawk homeobox) as potential gene targets of miR-6741-3p predicted by all the three algorithms (S3 Table). However, based on the literature survey, we first decided to check if miR-6741-3p can target *SRSF3* as the involvement of *SRSF3* in the pathogenesis of various cancers including OSCC has already been reported.

Validation of *SRSF3* as a gene target for miR-6741-3p

To check if *SRSF3* is indeed regulated by miR-6741-3p, we transfected the vector and pmiR-6741 constructs separately in SCC131 cells and assessed the levels of miR-6741-3p and the levels of *SRSF3* transcript and protein (Fig 2A). We observed that miR-6741-3p downregulated the level of SRSF3 protein while the level of *SRSF3* transcript remained unchanged in cells transfected with pmiR-6741 as compared to those transfected with the vector, suggesting that

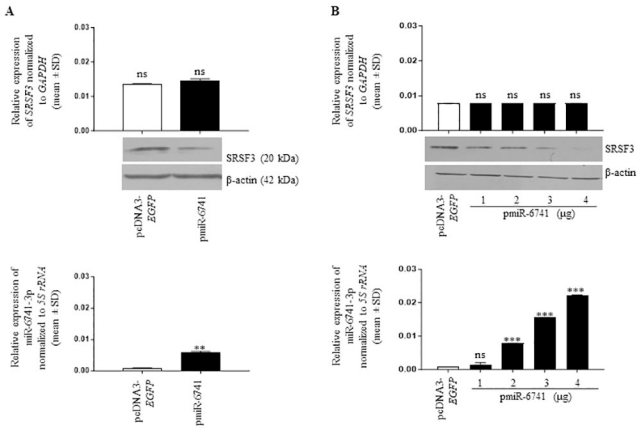

Fig 2. Identification of *SRSF3* as a gene target for miR-6741-3p. (A) SRSF3 protein level decreases, while the transcript level remains unchanged on overexpression of miR-6741-3p using the pmiR-6741 construct compared to the vector control. (B) A dose-dependent regulation of *SRSF3* at the translational level only is seen on increasing the doses of miR-6741-3p using the pmiR-6741 construct compared to the vector control. For qRT-PCR data, each bar is an average of 2 technical replicates.

https://doi.org/10.1371/journal.pone.0296565.g002

it regulates *SRSF3* expression at the translational level only (Fig 2A). We also transfected different quantities of the pmiR-6741 overexpression construct in SCC131 cells and analysed the expression of *SRSF3* by Western blotting and qRT-PCR. As expected, we observed that miR-6741-3p downregulated the level of *SRSF3* protein in a dose-dependent manner, while the level of *SRSF3* transcript remained unchanged (Fig 2B).

Confirmation of a direct interaction between miR-6741-3p and the 3'UTR of *SRSF3* by dual-luciferase reporter assay

Our bioinformatics analysis predicted one putative target site (TS) for the miR-6741-3p seed region (SR) in the 3'UTR of *SRSF3* from nucleotides 687–694, which is conserved across species (Fig 3A). The dual-luciferase reporter assay was performed to confirm the direct interaction between miR-6741-3p and the 3'UTR of *SRSF3* using different constructs illustrated in Fig 3B. The pMIR-REPORT-*SRSF3*-3'UTR construct with the 3'UTR of *SRSF3* in a sense orientation harbors the TS for miR-6741-3p. The negative control construct, pMIR-REPORT-*SRSF3*-3'UTR-M, is generated by abrogating the TS for miR-6741-3p in the 3'UTR of *SRSF3* by site-directed mutagenesis. To confirm if miR-6741-3p binds directly to the 3'UTR of *SRSF3* and to underscore the importance of the predicted TS, we co-transfected SCC131 cells separately with pMIR-REPORT-*SRSF3*-3'UTR-S and pmiR-6741 or pMIR-REPORT-*SRSF3*-3'UTR-S and the vector pcDNA3-*EGFP* and quantified the luciferase reporter activity. Compared to cells co-transfected with pMIR-REPORT-*SRSF3*-3'UTR-S and pcDNA3-*EGFP*, we observed a significant decrease in luciferase activity in those co-transfected with pMIR-REPORT-*SRSF3*-3'UTR-S and pmiR-6741, confirming that miR-6741-3p binds to the 3'UTR of *SRSF3* in a sequence-specific manner (Fig 3C). Further, as expected, cells co-transfected with pmiR-6741 and pMIR-REPORT-*SRSF3*-3'UTR-M showed luciferase activity comparable to those co-transfected with pMIR-REPORT-*SRSF3*-3'UTR-S and pcDNA3-*EGFP* due to the absence of miR-6741-3p TS in the pMIR-REPORT-*SRSF3*-3'UTR-M construct (Fig 3C). These observations suggested that miR-6741-3p binds to the TS in the 3'UTR of *SRSF3* directly in a sequence-specific manner.

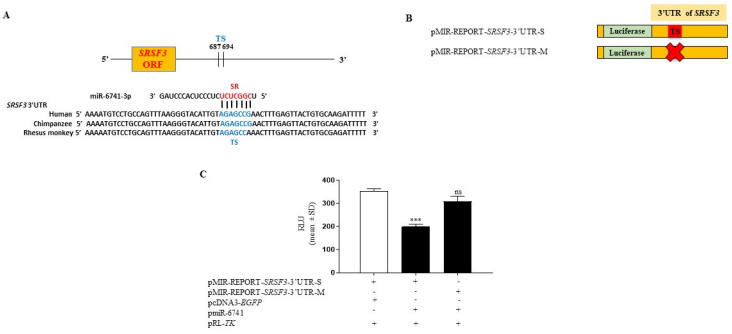

Fig 3. Confirmation of a direct interaction between miR-6741-3p and the 3'UTR of *SRSF3* by the dual-luciferase reporter assay in SCC131 cells. (A) Conservation of the putative target site (TS) for the miR-6741-3p seed sequence (SR) in the 3'UTR of *SRSF3* across species. (B) Schematic diagrams of different constructs for 3'UTR of *SRSF3* used in the dual-luciferase reporter assay. The 'X' in pMIR-REPORT-*SRSF3*-3'UTR-M indicates mutated TS. The "S" in pMIR-REPORT-*SRSF3*-3'UTR-S refers to "sense-strand" of 3'UTR of *SRSF3* with TS. (C) The results of dual-luciferase reporter assay. Note, reduced RLU in cells co-transfected with pMIR-REPORT-SRSF3-3'UTR-S and pmiR-6741 compared to those transfected with pMIR-REPORT-SRSF3-3'UTR-S and pcDNA3-EGFP. Each bar is an average of 3 biological replicates. Abbreviation: RLU, relative light unit.

https://doi.org/10.1371/journal.pone.0296565.g003

5-Azacytidine treatment of SCC131 cells upregulates miR-6741-3p expression and downregulates SRSF3

As mentioned earlier, miR-6741-3p was found to be significantly upregulated in 5-Azacytidine-treated SCC131 cells compared to the vehicle control-treated cells (Fig 1C). Since *SRSF3* was identified as the gene target for miR-6741-3p, we next checked the levels of both *SRSF3* transcript and protein in 5-Azacytidine and vehicle control-treated SCC131 cells. As expected, the level of SRSF3 protein was reduced with a concomitant increase in the level of miR-6741-3p in 5-Azacytine treated cells as compared to vehicle control-treated cells (S2 Fig), while no change in the level of *SRSF3* transcript was observed in 5-Azacytidine-treated cells as compared to vehicle control-treated cells (S2 Fig). These observations further underscore the importance of miR-6741-3p-mediated regulation of *SRSF3*.

Physiological relevance of the interaction between miR-6741-3p and *SRSF3* in cell lines and OSCC patient samples

As mentioned above, the regulation of *SRSF3* by miR-6741-3p is at the translational level. To check the physiological relevance of their interaction, we checked the levels of both miR-6741-3p and SRSF3 protein across seven different cell lines, namely SCC131, SCC084, A549, HeLa, HEK293T, U87, and MCF-7, and in 36 matched normal oral tissue and OSCC samples from patients. In general, an inverse correlation was observed between the expression of miR-6741-3p and SRSF3 across the cell lines that we have tested, indicating that this interaction is of physiological relevance (S3 Fig). For example, the level of miR-6741-3p is highest in U87 cells with almost no expression of SRSF3 protein (S3 Fig).

In the case of the OSCC patient samples, miR-6741-3p was found to be significantly downregulated in 16/36 tumor samples (viz., patient no. 3, 8, 33, 46, 49, 56, 64, 2, 5, 6, 10, 17, 31, 45, 48, and 59) as compared to their matched normal oral tissues (S4 Fig, upper panel).Additionally, we found SRSF3 to be upregulated in 12/36 OSCC samples (viz., patient no. 54, 3, 8, 33, 49, 53, 62, 2, 43, 51, 57, and 66) as compared to matched normal oral tissues (S4 Fig, lower panel).

Furthermore, miR-6741-3p was upregulated in 16/36 OSCC samples (viz., patient no. 54, 68, 47, 52, 53, 55, 14, 32, 43, 44, 50, 51, 60, 61, 65, and 67) as compared to matched normal oral tissues. In 4/36 samples (viz., patient no. 63, 62, 57, and 66), there was no change in the level of miR-6741-3p between normal oral tissue and tumors (S4 Fig, upper panel).Moreover, SRSF3 was found to be downregulated in 24/36 OSCC samples (viz., patient no. 63, 68, 46, 47, 52, 55, 56, 64, 5, 6, 10, 14, 17, 31, 32, 44, 45, 48, 50, 59, 60, 61, 65, and 67) as compared to matched normal oral tissues (S4 Fig, lower panel).

Overall, an inverse correlation was observed between the levels of miR-6741-3p and SRSF3 in 17/36 (47.22%; patient no. 68, 3, 8, 33, 47, 49, 52, 55, 2, 14, 32, 44, 50, 60, 61, 65, and 67) matched OSCC patient samples analyzed (S4 Fig).

SRSF3 overexpression increases cell proliferation

To study the role of *SRSF3* in various aspects of cancerous cells like proliferation, apoptosis, and anchorage-independent growth, we generated the p*SRSF3* overexpression construct. Using the same, the effect of *SRSF3* overexpression on proliferation of SCC131 and SCC084 cells was checked using the trypan blue dye exclusion assay. It was observed that *SRSF3* overexpressing cells showed increased cell proliferation compared to those transfected with the vector control in both the cell lines, suggesting that *SRSF3* positively regulates cell proliferation (S5 Fig).

Expression of SRSF3 depends on the presence or absence of its 3'UTR

To check the effect of miR-6741-3p-mediated regulation of *SRSF3* on its expression and function, we generated two different *SRSF3* constructs by inserting the 3'UTR of *SRSF3* downstream to the *SRSF3*-ORF in the p*SRSF3* construct. The two *SRSF3* constructs are as follows: p*SRSF3*-3'UTR-S containing the *SRSF3* ORF with its wild-type 3'UTR in a sense orientation and thus harboring a functional target site (TS) for miR-6741-3p binding, and p*SRSF3*-3'UTR-M containing the *SRSF3* ORF with the mutated TS in its 3'UTR in a sense orientation. We then co-transfected both SCC131 and SCC084 cells with pmiR-6741 and different *SRSF3* overexpression constructs or the vector control and performed the Western blot analysis (S6 Fig). The results showed that as compared to cells transfected with the vector control only, cells co-transfected with the vector and pmiR-6741 showed a decreased level of SRSF3 due to the targeting of endogenous SRSF3 by miR-6741-3p (S6 Fig). The level of SRSF3 increased in cells co-transfected with p*SRSF3* and pmiR-6741 as compared to those co-transfected with vector and pmiR-6741 (S6 Fig). The level of SRSF3 was decreased in cells co-transfected with p*SRSF3*-3'UTR-S and pmiR-6741 as compared to those co-transfected with p*SRSF3* and pmiR-6741, because of the presence of a functional TS in the 3'UTR of p*SRSF3*-3'UTR-S. The level of SRSF3 was rescued in cells co-transfected with p*SRSF3*-3'UTR-M and pmiR-6741 as compared to those co-transfected with p*SRSF3*-3'UTR-S and pmiR-6741, due to the presence of a mutated TS in the 3'UTR of p*SRSF3*-3'UTR-M (S6 Fig). These observations suggested that the expression of *SRSF3* depends on the presence or absence of its 3'UTR and is, in part, regulated by miR-6741-3p.

miR-6741-3p regulates cell proliferation and anchorage-independent growth, in part, by targeting the 3'UTR of *SRSF3*

To elucidate the effect of miR-6741-3p-mediated regulation of *SRSF3* on cell proliferation, we co-transfected different *SRSF3* overexpression constructs along with pmiR-6741 or vector control in both SCC131 and SCC084 cells and performed the trypan blue dye exclusion assay. As expected, we observed decreased proliferation of SCC131 cells co-transfected with vector and pmiR-6741 as compared to those transfected with vector only (Fig 4A). Cells co-transfected with pmiR-6741 and p*SRSF3*-3'UTR-S showed decreased cell proliferation as compared to those co-transfected with pmiR-6741 and p*SRSF3*, due to the presence of a functional target site (TS) for miR-6741-3p binding in the 3'UTR of p*SRSF3*-3'UTR-S (Fig 4A). As expected, no difference in cell proliferation was observed in cells co-transfected with pmiR-6741 and p*SRSF3* as compared to those co-transfected with pmiR-6741 and p*SRSF3*-3'UTR-M, due to the absence of a functional TS in 3'UTR of p*SRSF3*-3'UTR-M (Fig 4A). Similar results were obtained in SCC084 cells (Fig 4A). The above observations indicate that miR-6741-3p negatively regulates cell proliferation, in part, by targeting the 3'UTR of *SRSF3*.

Next, to analyse the effect of miR-6741-3p-mediated regulation of *SRSF3* on anchorage-independent growth capabilities of cells, we co-transfected different *SRSF3* overexpression constructs with pmiR-6741 or vector control in both SCC131 and SCC084 cells and performed the soft agar colony-forming assay. We used microscopic examination to score for visible colonies at the end of the experiment. As expected, we observed a sharp decrease in the number of colonies in SSC131 cells co-transfected with pmiR-6741 and the vector as compared to those transfected with vector only (Fig 4B). Further, SCC131 cells co-transfected with pmiR-6741 and p*SRSF3*-3'UTR-S construct harboring a functional TS for miR-6741-3p showed a decrease in the number of colonies compared to those co-transfected with p*SRSF3* and pmiR-6741 (Fig 4B). As expected, no significant difference in the number of colonies was observed in SCC131 cells co-transfected with pmiR-6741 and p*SRSF3* as compared to those co-transfected with

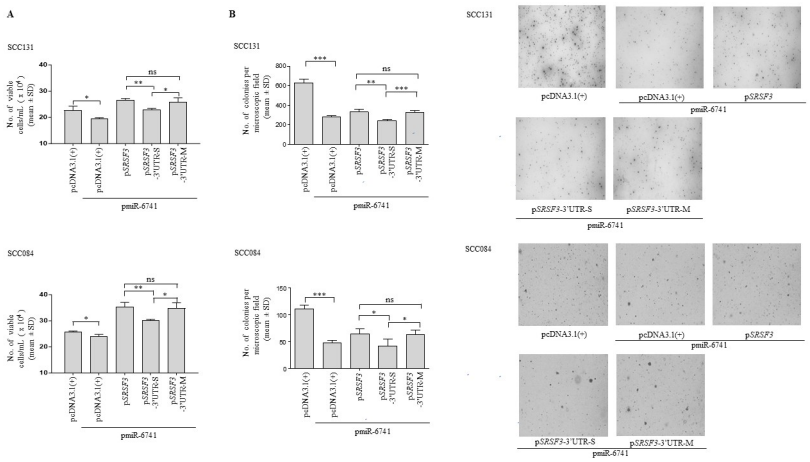

Fig 4. miR-6741-3p regulates cell proliferation and anchorage-independent growth, in part, by targeting the 3'UTR of *SRSF3*. (A) Quantitative analysis of cell proliferation by the trypan blue dye exclusion assay in SCC131 and SCC084 cells co-transfected with pmiR-6741 and different *SRSF3* overexpression constructs or vector control. (B) Quantitative assessment of the anchorage-independent growth capabilities and representative microphotographs of the colonies for SCC131 (upper panel) and SCC084 (lower panel) cells co-transfected with pmiR-6741 and different *SRSF3* overexpression constructs or vector control by the soft agar colony-forming assay. Each bar is an average of 4 biological replicates.

https://doi.org/10.1371/journal.pone.0296565.g004

pmiR-6741 and p*SRSF3*-3'UTR-M construct harboring a non-functional miR-6741-3p TS (Fig 4B). A similar observation was made in SCC084 cells also (Fig 4B). These observations clearly suggest that miR-6741-3p negatively regulates anchorage-independent growth, in part, by targeting the 3'UTR of *SRSF3*.

miR-6741-3p induces cellular apoptosis independent of *SRSF3*

Using different *SRSF3* overexpression constructs along with pmiR-6741 or vector control, we also analysed the effect of miR-6741-3p-mediated regulation of *SRSF3* on cellular apoptosis in both SCC131 and SCC084 cells. We observed that in both the cell lines, co-transfection of pmiR-6741 with the vector or any of the *SRSF3* constructs led to a significant increase in apoptosis as indicated by an increase in the percentage of Caspase-3 positive cells compared to only vector-transfected cells (Fig 5A), suggesting that miR-6741-3p positively regulates apoptosis. However, no difference in the percentage of apoptotic cells was found among cells transfected with any of the *SRSF3* constructs and pmiR-6741 (Fig 5A), suggesting that *SRSF3* has no effect on apoptosis. This was further confirmed by transfecting the vector or the p*SRSF3* construct separately in cells from both the cell lines and assessing the Caspase-3 activity. The results showed no change in the percentage of apoptotic cells between vector control and p*SRSF3* transfected cells (Fig 5B). These observations suggest that miR-6741-3p induces cellular apoptosis in both SCC131 and SCC084 cells independent of *SRSF3*.

Optimization of dosage for miR-6741-3p mimic and inhibitor in SCC131 cells

We wanted to explore the potential of a synthetic miR-6741-3p mimic and an inhibitor in regulating the levels of SRSF3. To this end, we transfected SCC131 cells with different quantities of mimic and inhibitor for optimization of the dosage. The results showed that 1,500 nM of miR-6741-3p mimic was sufficient to decrease the level of SRSF3 in SCC131 cells (S7A Fig). In

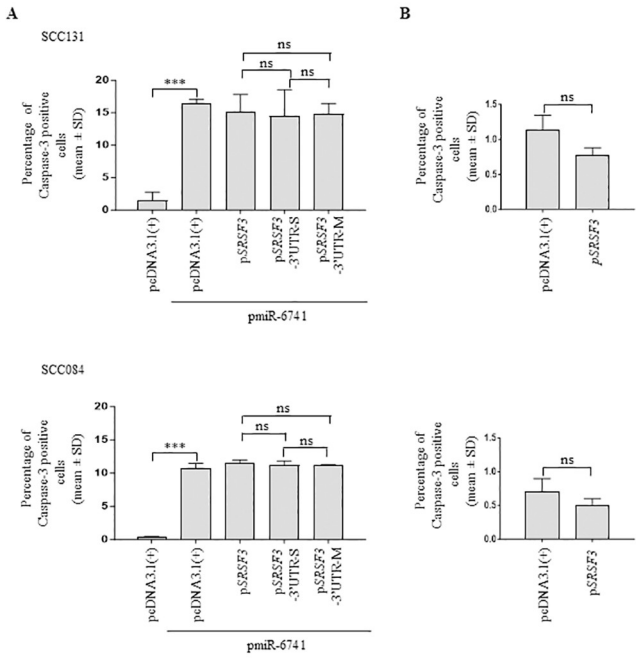

Fig 5. miR-6741-3p induces apoptosis independent of *SRSF3*. (A) Quantitative analysis of the apoptotic activity as assessed by the percentage of Caspase-3 positive cells in SCC131 (upper panel) and SCC084 (lower panel) cells co-transfected with pmiR-6741 and different *SRSF3* overexpression constructs or vector control. (B) No change in the apoptotic activity on overexpression of *SRSF3* compared to the vector control in both SCC131 (upper panel) and SCC084 (lower panel) cells. Each bar is an average of 3 biological replicates.

https://doi.org/10.1371/journal.pone.0296565.g005

the case of miR-6741-3p inhibitor, both 2,000 nM and 3,000 nM dosages were found to be effective in increasing the level of SRSF3 in SCC131 cells in a dose-dependent manner (S7B Fig). As expected, the qRT-PCR analysis showed an increased level of miR-6741-3p in mimic-treated cells and its decreased level in inhibitor-treated cells compared to those treated with controls, confirming their specificity (S7 Fig).

Restoration of miR-6741-3p by a mimic suppresses *in vivo* tumor growth, while its inhibition by an inhibitor promotes *in vivo* tumor growth in nude mice

Our *in vitro* studies hinted toward an anti-tumor activity of miR-6741-3p. Based on these observations, we hypothesized that the restoration of miR-6741-3p level by a synthetic miR-6741-3p mimic and, in turn, reducing the levels of SRSF3 in OSCC cells might have an anti-tumor effect *in vivo*. Conversely, decreasing the level of miR-6741-3p by a synthetic miR-6741-3p inhibitor and, in turn, increasing the level of SRSF3 in OSCC cells might promote tumor formation *in vivo*. We, therefore, decided to test this hypothesis using *in vivo* pre-treated OSCC xenograft nude mouse model. To this end, we injected equal numbers of SCC131 cells that were pre-transfected with 1,500 nM of miR-6741-3p mimic or 1,500 nM of mimic control separately into the right flanks of female nude mice. In another experimental set, we injected equal numbers of SCC131 cells that were pre-transfected with 3,000 nM of miR-6741-3p inhibitor or 3,000 nM of inhibitor control separately into the left flanks of the female nude mice. The mice were monitored for OSCC xenograft (tumor) growth until 26 days for the mimic group and 29 days for the inhibitor group. As expected, nude mouse xenografts with miR-

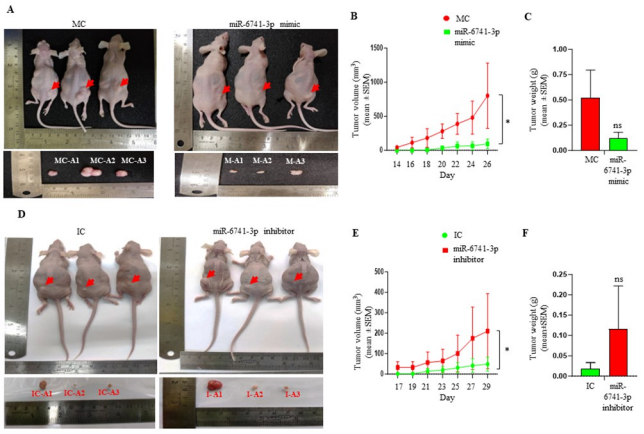

Fig 6. The effect of synthetic miR-6741-3p mimic and inhibitor on SCC131 cell-derived xenografts in nude mice. (A) Top panel: photographs of nude mice showing tumor growth after 26 days of injection of cells pre-treated with miR-6741-3p mimic and the control. Bottom panel: Excised xenografts from cells-pretreated with miR-6741-3p mimic and control on Day 26. (B) Effect of miR-6741-3p mimic on the volume of xenografts during a time course of 26 days. For mimic control group: n = 5, Day 14–22; n = 4, Day 24–26; and, for miR-6741-3p mimic group: n = 6. (C) Effect of miR-6741-3p mimic on the weight of xenografts on day 26. (D) Top panel: photographs of nude mice showing tumor growth after 29 days of injection of cells pre-treated with miR-6741-3p inhibitor and the control. Bottom panel: Excised xenografts from cell-pretreated with miR-6741-3p inhibitor and control on Day 29. (E) Effect of miR-6741-3p inhibitor on the volume of xenografts during a time course of 29 days. For inhibitor control group: n = 7; and, for miR-6741-3p inhibitor group: n = 7, Day 17–23; n = 6, Day 25–27; n = 5, Day 29. (F) Effect of miR-6741-3p inhibitor on the weight of xenografts on Day 29. Note, for tumor volume and weight measurements, all the animals alive at a particular data point were considered for data collection irrespective of tumor development. For miR-6741-3p mimic and the mimic control cohort, 6 animals were injected per group, and for miR-6741-3p inhibitor and inhibitor control cohort 7 animals were injected per group. Abbreviations: MC, mimic control; and, IC, inhibitor control.

https://doi.org/10.1371/journal.pone.0296565.g006

6741-3p mimic had significantly reduced volumes in comparison to those with control (Fig 6A and 6B). Also, the tumor weights were reduced in mice treated with miR-6741-3p mimic compared to those treated with mimic control; however, the difference was not statistically significant (Fig 6C). Similarly, as expected, nude mouse xenografts with miR-6741-3p inhibitor had significantly increased tumor volumes in comparison to those with inhibitor control (Fig 6D and 6E). As expected, the tumor weights were increased in mice treated with miR-6741-3p inhibitor compared to those treated with inhibitor control; however, the difference was not statistically significant (Fig 6F). Taken together, these observations suggest that miR-6741-3p inhibits tumor growth *in vivo*, in part, by targeting the 3'UTR of *SRSF3*.

Overexpression of miR-6741-3p leads to a decrease in activation, while overexpression of *SRSF3* leads to activation of the PI3K/AKT/MTOR and ERK/MAP pathways

The PI3K-AKT-MTOR pathway, a central hub for controlling cellular proliferation and growth, is the most frequently activated pathway in OSCC. Apart from this, the ERK/MAPK pathway is also frequently deregulated in various cancers including OSCC. We, therefore, decided to analyze the activation of these two critical pathways on overexpression of miR-6741-3p or *SRSF3*, using the Western blot analysis. As read-outs for the activated PI3K-AKT-MTOR pathway, we decided to check the levels of phospho- and total-S6K1. Similarly, we checked the levels of phospho- and total-ERK1/2 as read-outs for the activated ERK/MAPK signaling pathway. The results showed decreased levels of phospho- and total-S6K1 as well as phospho- and total-ERK1/2 levels in both SCC131 and SCC084 cells, following

overexpression of miR-6741-3p (S8A Fig). As expected, overexpression of miR-6741-3p led to a decreased level of SRSF3 in both SCC131 and SCC084 cells (S8A Fig). Overexpression of *SRSF3* on the other hand led to increased levels of phospho- and total-S6K1 as well as phospho- and total-ERK1/2 levels in both SCC131 and SCC084 cells (S8B Fig). The above observations suggest that miR-6741-3p decreases signaling through both the PI3K-AKT-MTOR and the ERK/MAPK pathways, in part, by regulating SRSF3, and there seems to be a miR-6741-3p-SRSF3-ERK1/2-S6K1 axis.

Putative *MIR6741* promoter lacks any promoter activity

We wanted to identify the mechanism for the upregulation of miR-6741-3p following the 5-Azacytidine treatment of SCC131 cells. We hypothesized that miR-6741-3p is upregulated following 5-Azacytidine treatment due to demethylation of its promoter.

To test this hypothesis, the putative *MIR6741* promoter sequence encompassing the proximal region of the *MIR6741* locus was retrieved from the DBTSS database [17] (S9A Fig) and cloned in the pGL3-Basic vector, a promoterless vector. To check if additional regulatory sequences are needed for the promoter to function, we generated another construct (pmiR-6741-F2) by cloning a larger fragment that encompassed the predicted putative promoter sequence along with additional upstream and downstream sequences (S9B Fig). The two constructs for the putative *MIR6741* promoter are schematically represented in S9C Fig. The two putative promoter constructs (pmiR-6741-F1 and pmiR-6741-F2) along with the control pGL3-Control and pGL3-Basic were then transfected separately in SCC131 cells and the dual-luciferase reporter assay was performed. However, the results showed no promoter activity for both the putative *MIR6741* promoter constructs (S10 Fig), indicating that the proximal region of the *MIR6741* locus does not represent the *MIR6741* promoter.

Discussion

The present study was focused on the identification of novel tumor suppressor miRNAs involved in OSCC pathogenesis at a genome-wide scale. The microRNA microarray analysis of cells from an OSCC cell line SCC131 treated with 5-Azacytidine and vehicle control (DMSO) led to the identification of 50 upregulated and 28 downregulated miRNAs (Fig 1B, S1 Table). miR-6741-3p was one of the 50 upregulated miRNAs (tumor suppressors) that was validated by qRT-PCR (Fig 1B and 1C) and studied in detail. It is a poorly conserved intronic miRNA present in the intron between exons 3 and 4 of the transcript variant I of the host gene *PYCR2* (Pyrroline-5-carboxylate reductase family, member2) and was discovered recently by Ladewig and co-workers [18]. The physiological function of this miRNA has not been annotated and there are very few reports of its involvement in disease conditions [19, 20].

Like the classical tumor suppressor genes, one of the defining characteristics of a tumor suppressor miRNA is its ability to suppress the proliferation of cancer cells. In our study, the overexpression of miR-6741-3p in SCC131 and SCC084 cells decreased cell proliferation, confirming its tumor-suppressive nature (S1 Fig). Tumor suppressor miRNAs exert their effect through the repression of their target oncogenic mRNA networks, leading to an inhibition of tumorigenesis [21]. Using bioinformatics analysis, the oncogene *SRSF3* was identified as a potential target for miR-6741-3p (S3 Table). In this study, we showed for the first time that the overexpression of miR-6741-3p downregulated *SRSF3* at the protein level in OSCC cells, but there was no change at the RNA level, indicating that translational inhibition and not mRNA degradation is involved in miR-6741-3p-mediated suppression of *SRSF3* (Fig 2). Using a combination of computational prediction and dual-luciferase reporter assay, we established that

the oncogene *SRSF3* is indeed an evolutionarily conserved direct target for miR-6741-3p (Fig 3).

SRSF3 is a multifunctional protein belonging to the SR family of proteins and apart from its classical role in regulating constitutive and alternative splicing, it also regulates several cellular processes like mRNA export, alternative polyadenylation, miRNA biogenesis, transcription termination, DNA repair, nuclear RNA quality control, stress granule assembly, maintenance of transcriptome integrity of developing oocytes and regulation of pluripotency [22]. It promotes tumorigenesis by regulating the expression of a plethora of protein-coding genes as well as miRNAs that are directly involved in carcinogenesis [23–26]. It is overexpressed in a wide variety of cancers like cancers of the lungs, skin, stomach, liver, cervix, bladder, breasts, colon, kidneys, thyroid, ovaries, various mesenchymal tissues as well as OSCC [27–29]. Gene amplification and impairment of *SRSF3* autoregulation have been attributed to its overexpression in at least a subset of these cancers [27, 30]. As we identified *SRSF3* as a direct target for miR-6741-3p, we proposed that the downregulation of miR-6741-3p might also be responsible for the increased expression of SRSF3 in OSCC and other cancers and might play a critical role in tumorigenesis. Our finding of an inverse correlation between the expression of miR-6741-3p and SRSF3 in various cell lines (S3 Fig) and a subset (17/36; 47.22%) of paired normal oral tissue and OSCC samples (S4 Fig) supported that indeed miR-6741-3p-mediated regulation of *SRSF3* is of physiological and biological relevance. However, we were not able to observe any correlation in 19/36 (52.78%) OSCC patient samples. The lack of correlation in the levels of miR-6741-3p and SRSF3 in these OSCC samples could be attributed to factors like tumor heterogeneity, splicing factors redundancy, involvement of additional levels of regulation of *SRSF3*, variable etiopathogenesis, and heterogeneous genetic constitution of each patient [31]. Similar discrepancies in the expression of miRNAs and their target genes across different studies have been reported earlier. For example, Mallela et al. [32] found an inverse correlation in the levels of miR-130a and its target gene *TSC1* in 19/36 (52.78%) OSCC samples only. Rather et al. [33] observed an inverse correlation in the levels of miR-155 and its target gene *CDC73* in 10/18 (55.56%) OSCC samples only.

Given the fact that SRSF3 is overexpressed in multiple cancers, including OSCC and acts as an oncogene, we decided to investigate how miR-6741-3p-mediated regulation of *SRSF3* affects its oncogenic function in OSCC cells *in vitro* and *in vivo*. To assess the same, we incorporated the sense and mutant 3'UTR of *SRSF3* downstream to the *SRSF3* ORF in the p*SRSF3* construct and co-transfected these constructs (p*SRSF3*-3'UTR-S and p*SRSF3*-3'UTR-M) separately in OSCC cells with pmiR-6741. This approach helped us to concurrently confirm that the change in expression of *SRSF3* is due to the interaction between its 3'UTR and miR-6741-3p and analyzed the effect of this interaction on the oncogenic function of SRSF3. The Western blot analysis revealed that the presence of the wild-type 3'UTR and not the mutant 3'UTR in the expression vector dramatically inhibited the production of SRSF3 protein (S6 Fig) in miR-6741-overexpressing OSCC cells, indicating that the expression of *SRSF3* is modulated by the interaction of miR-6741-3p with its 3'UTR. We then co-transfected all the *SRSF3* constructs (p*SRSF3*, p*SRSF3*-3'UTR-S, and p*SRSF3*-3'UTR-M) along with the pmiR-6741 construct and investigated if the miR-6741-3p-mediated knockdown of *SRSF3* is reflected on cell proliferation, anchorage-independent growth, and apoptosis of OSCC cells (Figs 4 and 5). In the presence of the pmiR-6741 construct, the overexpression of SRSF3 protein using the constructs without its 3'UTR (p*SRSF3*) or with the mutated 3'UTR (p*SRSF3*-3'UTR-M) promoted the proliferation and anchorage-independent growth of OSCC cells (Fig 4). This is in line with other studies where the overexpression of SRSF3 promoted proliferation and anchorage-independent growth of cancer cells, while the knockdown of *SRSF3* suppressed proliferation and anchorage-independent growth [27, 28, 34]. However, contrary to the earlier studies [27,

28, 35, 36] which demonstrated the anti-apoptotic property of SRSF3, in our study, overexpression of SRSF3 protein using any of the three constructs was not able to rescue miR-6741-3p-induced apoptosis, indicating that SRSF3 has no effect on apoptosis of OSCC cells (Fig 5). Taken together, the *in vitro* studies demonstrated that miR-6741-3p suppresses proliferation and anchorage-independent growth of OSCC cells, in part, by targeting the 3'UTR of *SRSF3*, and promotes apoptosis of OSCC cells independent of *SRSF3*.

We have further confirmed the tumor-suppressive properties of miR-6741-3p in oral cancer using an *in vivo* pre-treatment OSCC xenograft nude mice model system. In our study, we demonstrated that restoration of miR-6741-3p by a mimic suppresses *in vivo* tumor growth, while its inhibition by an inhibitor promotes *in vivo* tumor growth in nude mice. (Fig 6). Though the observed differences in tumor volume between miR-6741-3p mimic and mimic control-treated group, as well as, miR-6741-3p inhibitor and inhibitor control-treated groups were reflected in tumor weights, the difference was not statistically significant (Fig 6C and 6F. This limitation of the present study can be attributed to inter-animal variation in tumor weights, which in turn was largely due to variation in time required for tumor induction in our animal cohort.

Lastly, in a bid to identify the molecular effectors and pathways affected by miR-6741-3p-mediated regulation of *SRSF3* in OSCC, we focused on two critical pathways namely, PI3K-AKT-MTOR and ERK/MAPK which are frequently deregulated in OSCC and other cancers [37–39]. Our results demonstrated that there is a miR-6741-3p-SRSF3-ERK1/2-S6K1 axis through which miR-6741-3p decreases signaling, in part, by modulating SRSF3 (S8 and S11 Figs). Taken together, our findings from the *in vitro* and *in vivo* assays not only highlight the oncogenic role of SRSF3 during oral carcinogenesis, but also strongly attest to the tumor-suppressive role of miR-6741-3p in OSCC, in part, by targeting *SRSF3*.

Early reports suggested that transcription of intronic miRNAs is linked to the host gene transcription and requires RNA Pol II and splicing machinery for their biogenesis [40, 41]. However, Monteys et al. [42] predicted that ~35% of intronic miRNAs can be transcribed from independent promoters by Pol II or Pol III. The increase in expression of miR-6741-3p following 5-Azacytidine treatment of SCC131 cells (Fig 1B and 1C) therefore could be attributed to the demethylation at the *MIR6741* promoter if *MIR6741* has its independent promoter. In our study, *MIR6741* promoter constructs (pmiR-6741-F1 and pmiR-6741-3p-F2) that we generated based on the prediction by the DBTSS database were not able to drive the expression of the luciferase reporter (S9 and S10 Figs), indicating that *MIR6741* lacks an independent promoter. We will be thus exploring the underlying mechanism of miR-6741-3p upregulation following 5-Azacytidine treatment of SCC131 cells in the future.

In summary, our study identified for the first time a total of 50 potential tumor suppressor miRNAs in OSCC on a genome-wide scale. The current study clearly demonstrated that the oncogene *SRSF3* is a target for the tumor suppressor miR-6741-3p. We substantiate this conclusion with a combination of *in silico*, *in vitro*, and *in vivo* assays. Further, we suggest that the restoration of miR-6741-3p level by using a synthetic miR-6741-3p mimic could be a potent strategy to treat OSCC and perhaps other cancers.

Materials and methods

Cell lines

UPCI: SCC131 (SCC131) and UPCI: SCC084 (SCC084) cell lines are a kind gift from Dr. Susanne M. Gollin (University of Pittsburgh, Pittsburgh, PA, USA) [43]. HeLa, A549 and HEK293T cells were procured from the cell repository, National Centre for Cell Sciences,

Pune, India. U87 and MCF-7 cell lines were obtained from Prof. P. Kondaiah's laboratory, Department of Developmental Biology and Genetics, IISc, Bengaluru, India.

5-Azacytidine treatment and miRNA microarray analysis

SCC131 cells were treated separately with 5 μM 5-Azacytidine for 5 days (cat# A1287; Sigma-Aldrich, St. Louis, MO, USA) and vehicle control DMSO (cat# D4540; Sigma-Aldrich, St. Louis, MO, USA), following a standardized laboratory protocol. Following this, the expression of 2,459 mature miRNAs was investigated by the microRNA microarray analysis using SurePrint G3 8x60K Human miRNA Microarray chips (AMADID 70156; Agilent Technologies, Santa Clara, CA, USA).

In silico identification of targets for miR-6741-3p

Three target prediction programs, namely miRDB [44], DIANA-microT-CDS [45, 46] and TargetScan [47] were used to identify target genes for miR-6741-3p (S3 Table).

Sample collection

A total of 36 matched normal oral tissue and OSCC patient samples were ascertained at the Kidwai Memorial Institute of Oncology (KMIO), Bengaluru, from 13th July, 2018 to 14th November, 2018. The study was performed with written informed consent from the patients following approvals from the ethics committee of Kidwai Memorial Institute of Oncology, Bengaluru (approval # KMIO/MEC/021/05.January.2018). This study was conducted in accordance with principles of Helsinki declaration. The samples were obtained as surgically resected tissues from oral cancerous lesions and adjacent normal tissues (taken from the farthest margin of surgical resection) in the RNALater™ (Sigma-Aldrich, St. Louis, MO, USA) and transferred to -80˚C until further use. The tumors were staged according to the UICC's (International Union against Cancer) TNM (Tumor, Node, and Metastasis) classification [48]. The details of the clinicopathological parameters obtained from the patients are summarised in S4 Table.

Total RNA extraction and qRT-PCR

Total microRNA enriched RNA sample for microRNA microarray analysis was isolated using a mirVana™ miRNA isolation kit (cat# AM1561; Ambion, Austin, TX, USA), according to the manufacturer's protocol. Total RNA from cell lines and tissues was isolated using TRI Reagent™ (Sigma-Aldrich, St. Louis, MO, USA). RNA was quantitated using a NanoDrop™ 1000 spectrophotometer (Thermo Fisher Scientific, Waltham, MA, USA). First-strand cDNA synthesis was done using 1–2 μg of total RNA and a Verso cDNA Synthesis Kit (Thermo Fischer Scientific, Waltham, MA, USA). The expression of miR-6741-3p was determined as suggested by Sharbati-Tehrani et al. [49]. The qRT-PCR analysis was carried out using a DyNAmo ColorFlash SYBR Green qPCR Kit in a StepOnePlus Real-Time PCR System (Thermo Fischer Scientific, Waltham, MA, USA). *GAPDH* and *5S rRNA* were used as normalizing controls. The following equation, $\Delta Ct_{gene} = Ct_{gene}\text{-}Ct_{normalizing\ control}$, was used to calculate the fold change in expression. Ct represents cycle threshold value, and ΔCt represents the gene expression normalized to *GAPDH* or *5S rRNA*. A two-tailed unpaired t-test was performed using the GraphPad PRISM5 software (GraphPad Software Inc., San Diego, CA, USA) to analyze the statistical significance of the difference in mRNA expression. Details of the RT-PCR primers are given in S2 Table.

In silico identification of the putative MIR6741 promoter

The putative promoter sequence for *MIR6741* was retrieved by an *in silico* search using the DBTSS [17] database.

Plasmid constructs

miR-6741 (pmiR-6741) and *SRSF3* (p*SRSF3*) overexpression constructs were generated in the pcDNA3-*EGFP* and pcDNA3.1(+) vectors respectively, using human genomic DNA or human cDNA as templates as required and gene-specific PCR primers following a standard laboratory procedure (S5 Table). Different restriction enzyme sites were incorporated in forward and reverse primers to facilitate directional cloning.

To generate the pMIR-REPORT-*SRSF3*-3'UTR-S construct containing the 3'UTR of *SRSF3* at the 3' end of luciferase ORF in the pMIR-REPORT™ vector (Invitrogen, Waltham, MA, USA), fragments were amplified using specific primers and human genomic DNA as a template and cloned in a sense orientation using a standard laboratory method (S5 Table). The pMIR-REPORT-*SRSF3*-3'UTR-M construct containing the mutated target site in *SRSF3* 3'UTR was also generated by site-directed mutagenesis according to Sambrook et al. [50] using specific primers and pMIR-REPORT-*SRSF3*-3'UTR-S as the template (S6 Table). The p*SRSF3*-3'UTR-S and p*SRSF3*-3'UTR-M constructs carrying the wild-type (WT) and mutant (M) 3'UTR of *SRSF3* hooked downstream to the *SRSF3* ORF were generated by sub-cloning the wild-type and mutant *SRSF3* 3'UTR from pMIR-REPORT-*SRSF3*-3'UTR-S and pMIR-REPORT-*SRSF3*-3'UTR-M constructs respectively in the p*SRSF3* construct. Briefly, the *SRSF3*-3'UTR sense and mutant fragments were excised from the pMIR-REPORT-*SRSF3*-3'UTR-S and pMIR-REPORT-*SRSF3*-3'UTR-M constructs respectively by digestion with *Bam* HI and *Eco* RV restriction enzymes (S5 Table). The digested fragments were then ligated and cloned in the p*SRSF3* construct also digested by the same enzymes to ensure directional cloning to generate the p*SRSF3*-3'UTR-S and p*SRSF3*-3'UTR-M constructs.

To generate the pmiR-6741-F1 and pmiR-6741-F2 constructs used for promoter validation in the pGL3-Basic vector (Promega, Madison, WI, USA), fragments were amplified using specific primers and human genomic DNA as the template and cloned using a standard laboratory method (S5 Table). The details of the sequences used to generate the different *MIR6741* promoter constructs are given in S7 Table.

All the constructs used in the study were validated by restriction enzyme digestion and Sanger sequencing on a 3730xl DNA Analyzer (Thermo Fisher Scientific, Waltham, MA, USA).

Cell culture, transient transfection, and reporter assays

All the cell lines were maintained in Dulbecco's modified eagle medium (DMEM) supplemented with 10% (v/v) fetal bovine serum (FBS) and 1X antibiotic-antimycotic solution [DMEM and 1X antibiotic-antimycotic solution from Sigma-Aldrich, St. Louis, MO, USA; FBS from Thermo Fisher Scientific, Waltham, MA, USA)] in a humidified incubator with 5% CO_2 at 37˚C.

For overexpression studies, SCC131 or SCC084 cells were seeded at a density of 2×10^6 cells/well in a 6-well plate and transiently transfected with an appropriate construct or co-transfected with a combination of constructs using the Lipofectamine 2000 transfection reagent (Thermo Fisher Scientific, Waltham, MA, USA), following the manufacturer's protocol. Post 48 hr of transfection, total RNA and protein were isolated from the cells. The direct interaction between the 3'UTR of the target gene and miRNA as well as the promoter activity of the generated constructs was validated using the dual-luciferase reporter assay. Briefly,

5×10^4 cells/well were transfected with different constructs as mentioned above. The assay was carried out after 48 hr of transfection in SCC131 cells, using the Dual Luciferase® Reporter Assay System (Promega, Madison, WI, USA) and the VICTOR™ X Multilabel Plate Reader (PerkinElmer, Waltham, MA, USA) [33, 51]. The transfection efficiency in the dual-luciferase reporter assay was normalized by co-transfecting with the pRL-*TK* control vector [33, 51].

Western blot hybridization

Protein lysates from cell lines were prepared using the CelLytic™ M Cell Lysis Reagent (Sigma-Aldrich, St. Louis, MO, USA), while CelLytic™ MT Mammalian Tissue Lysis Reagent (Sigma-Aldrich, St. Louis, MO, USA) was used to prepare lysates from oral tissue samples. The proteins were resolved on SDS-PAGE and transferred onto a PVDF membrane (Pall Corp., Port Washington, NY, USA) using a locally made conventional semi-dry or wet transfer apparatus (Bio-Rad™, Hercules, CA, USA) as per the requirement. The membrane was blocked using 5% skimmed milk powder (Nestlé India Ltd., Gurgaon, India) in 1X PBS-Tween®20 buffer. The signal was visualized using appropriate primary and secondary antibodies and the Immobilon™ Western Chemiluminescent HRP substrate (Merck, Darmstadt, Germany) and developed on an X-ray film. The anti-mouse β-actin (1:10,000 dilution, cat# A5441; Sigma-Aldrich, St. Louis, MO, USA) was used as a loading control. An anti-SRSF3 antibody (1:2000 dilution, cat# ab198291) was purchased from Abcam (Cambridge, MA, USA). Antibodies such as anti-phospho-p44/42 MAPK (Erk1/2) (Thr202/Tyr204) (1:1000 dilution, cat# 9101), anti-p44/42 MAPK (Erk1/2) (1:1000 dilution, cat# 9102), anti-phospho-p70 S6 Kinase (Thr421/Ser424) (1:1000 dilution, cat# 9204) and anti-p70 S6 Kinase (1:1000 dilution, cat# 9202) were purchased from Cell Signaling Technology (Danvers, MA, USA). The anti-rabbit HRP-conjugated secondary antibody (1.5:5000 dilution, cat# HP03) and anti-mouse HRP-conjugated secondary antibody (1:5000 dilution, cat# HP06) were purchased from Bangalore Genei® (Bengaluru, India).

Cell proliferation assay

The rate of proliferation of SCC131 and SCC084 cells transfected with an appropriate construct or co-transfected with a combination of constructs was assessed by employing a trypan blue dye exclusion assay as described by Karimi et al. [52].

Apoptosis assay

The CaspGLOW™ Fluorescein Active Caspase-3 Staining kit (BioVision, Milpitas, CA, USA) was used to quantify the apoptosis of cells transfected with the appropriate constructs, according to the manufacturer's instructions, and as described by Mallella et al. [32].

Soft agar colony-forming assay

Tumor cells can overcome anoikis to proliferate and form colonies in suspension within a semi-solid medium such as soft agar [53]. The anchorage-independent growth of cells co-transfected with a combination of constructs was analysed by the soft agar colony-forming assay in 35 mm tissue culture dishes, following a standard laboratory protocol [33].

In vivo assay for tumor growth

The tumor-suppressive property of miR-6741-3p was investigated using an *in vivo* nude mice OSCC xenograft model. The effect of miR-6741-3p overexpression using a synthetic miR-6741-3p mimic and a synthetic miR-6741-3p inhibitor on tumor growth was assayed in 4–6

weeks old female NU/J athymic nude mice. Briefly, 2×10^6 SCC131 cells were transfected with 1,500 nM of mimic control or miR-6741-3p mimic. Post 24 hr of transfection, 2×10^6 cells were suspended in 150 μL DPBS and then subcutaneously injected into the right posterior flank of each mouse. The same method was used to inject SCC131 cells transfected with 3,000 nM of inhibitor control or miR-6741-3p inhibitor into the left posterior flank of each mouse. Tumors were allowed to grow in animals of all the four experimental sets, and tumor volumes were measured using a Vernier's caliper every alternate day till the termination of the experiment. At the end of the study, animals were euthanized under sterile conditions and under CO_2 atmosphere by cervical dislocation by a trained personnel. Tumor volumes were calculated using the formula: $V = L\times W^2\times0.5$, where L and W represent the length and width of the tumor respectively. The animals were photographed, and the tumor xenografts were harvested at the end of the study. Harvested xenografts were also photographed and weighed. This study was carried out in strict accordance with the recommendations in the Guide for the Care and Use of Laboratory Animals of the National Institutes of Health and ARRIVE guidelines. The protocol was approved by the Institutional Animal Ethics Committee on the Ethics of Animal Experiments of the Indian Institute of Science, Bengaluru (approval certificate # project proposal no. 766, dated October 08,2020). All surgery was performed under isoflurane anesthesia, and all efforts were made to minimize suffering of animals. All mice were maintained on a 12:12 h light/dark cycle in proper cages with sufficient food and water. During the course of the study, efforts were taken to alleviate suffering, animals were handled and treated only by a trained personnel, and all animals were consistently monitored for general health and behaviour. The miRNA mimics and inhibitors used in the study-miRIDIAN microRNA hsa-miR-6741-3p-Mimic (cat# C-302786-00-0020), miRIDIAN microRNA hsa-miR-6741-3p-Hairpin Inhibitor (cat# IH-302786-01-0020), miRIDIAN microRNA Mimic Negative Control #1 (cat# CN-001000-01-20), and miRIDIAN microRNA Hairpin Inhibitor Negative Control #1 (cat# IN-001005-01-20)-were all purchased from Dharmacon (Lafayette, CO, USA). All experiments were carried out in accordance with relevant guidelines and regulations.

Statistical analysis

A two-tailed student's *t*-test was performed using the GraphPad PRISM5 software (GraphPad Software Inc., San Diego) to analyze the statistical significance of the difference between two data sets. Differences with P-value ≤0.05 (*), P-value <0.01 (**), and P-value <0.001 (***) were considered statistically significant, whereas P-value >0.05 was considered as statistically non-significant (ns).

Supporting information

S1 Fig. miR-6741-3p decreases the proliferation of SCC131 and SCC084 cells.
(PDF)

S2 Fig. 5-Azacytidine treatment of SCC131 cells upregulates miR-6741-3p expression and downregulates SRSF3.
(PDF)

S3 Fig. Expression analysis of miR-6741-3p and SRSF3 in cell lines.
(PDF)

S4 Fig. Expression analysis of miR-6741-3p and SRSF3 in OSCC patient samples.
(PDF)

S5 Fig. SRSF3 overexpression increases the proliferation of SCC131 and SCC084 cells.
(PDF)

S6 Fig. SRSF3 expression depends on the presence or absence of its 3'UTR.
(PDF)

S7 Fig. Optimization of dosage for miR-6741-3p mimic and inhibitor in SCC131 cells.
(PDF)

S8 Fig. MiR-6741-3p decreases signaling through both PI3K-AKT-MTOR and ERK/MAPK pathways, in part, by regulating SRSF3.
(PDF)

S9 Fig. Putative promoter sequence for the *MIR6741* gene.
(PDF)

S10 Fig. The dual-luciferase reporter assay for putative *MIR6741* promoter fragments in SCC131 cells.
(PDF)

S11 Fig. Effect of miR-6741-3p-mediated regulation of SRSF3 on the PI3K/AKT/MTOR and the ERK/MAPK pathways.
(PDF)

S1 Table. Differentially expressed microRNAs identified by microRNA microarray analysis of 5-Azacytidine and DMSO-treated SCC131 cells.
(PDF)

S2 Table. Details of primers used in qRT-PCR.
(PDF)

S3 Table. A list of predicted gene targets^ for miR-6741-3p.
(PDF)

S4 Table. Clinicopathological parameters of the patients included in the study.
(PDF)

S5 Table. Details of plasmid constructs used in the study.
(PDF)

S6 Table. Details of construct generated by site-directed mutagenesis in the study.
(PDF)

S7 Table. Details of the putative *MIR6741* promoter fragments cloned in the pGL3-Basic vector.
(PDF)

S1 Raw images.
(PDF)

Acknowledgments

We are grateful to the patients for providing the normal and tumor oral samples. We thank three anonymous reviewers for their comments and suggestions to improve the quality of the manuscript.

Author Contributions

Conceptualization: Arun Kumar.

Data curation: Dhanashree Anil More.

Formal analysis: Dhanashree Anil More.

Funding acquisition: Arun Kumar.

Investigation: Dhanashree Anil More, Nivedita Singh, Harsha Pulakkat Muralidharan.

Methodology: Dhanashree Anil More, Nivedita Singh, Radha Mishra, Champaka Gopal.

Project administration: Kodaganur Srinivas Gopinath, Arun Kumar.

Resources: Radha Mishra, Kodaganur Srinivas Gopinath, Champaka Gopal, Arun Kumar.

Supervision: Arun Kumar.

Validation: Dhanashree Anil More, Nivedita Singh.

Visualization: Dhanashree Anil More.

Writing – original draft: Dhanashree Anil More.

Writing – review & editing: Arun Kumar.

References

1. Massano J, Regateiro FS, Januário G, Ferreira A. Oral squamous cell carcinoma: Review of prognostic and predictive factors. Oral Surg Oral Med Oral Pathol Oral Radiol Endod. 2006 Jul; 102(1):67–76. https://doi.org/10.1016/j.tripleo.2005.07.038 PMID: 16831675
2. *GLOBOCAN 2020*: *New Global Cancer Data*. https://www.uicc.org/news/globocan-2020-new-global-cancer-data (2020).
3. Sung H, Ferlay J, Siegel RL, Laversanne M, Soerjomataram I, Jemal A, et al. Global Cancer Statistics 2020: GLOBOCAN estimates of incidence and mortality worldwide for 36 cancers in 185 countries. CA Cancer J Clin. 2021 May; 71(3):209–249. https://doi.org/10.3322/caac.21660 PMID: 33538338
4. Bonner JA, Harari PM, Giralt J, Cohen RB, Jones CU, Sur RK, et al. Radiotherapy plus cetuximab for locoregionally advanced head and neck cancer: 5-year survival data from a phase 3 randomised trial, and relation between cetuximab-induced rash and survival. Lancet Oncol. 2010 Jan; 11(1):21–8. https://doi.org/10.1016/S1470-2045(09)70311-0 PMID: 19897418
5. Omar E. Current concepts and future of noninvasive procedures for diagnosing oral squamous cell carcinoma-A systematic review. Head Face Med. 2015 Mar; 11:6. https://doi.org/10.1186/s13005-015-0063-z PMID: 25889859
6. Ameres SL, Zamore PD. Diversifying microRNA sequence and function. Nat Rev Mol Cell Biol. 2013 Aug; 14(8):475–88. https://doi.org/10.1038/nrm3611 PMID: 23800994
7. Chakraborty C, Sharma AR, Sharma G, Lee SS. Therapeutic advances of miRNAs: A preclinical and clinical update. J Adv Res. 2020 Aug; 28:127–138. https://doi.org/10.1016/j.jare.2020.08.012 PMID: 33364050
8. D'Souza W, Kumar A. MicroRNAs in oral cancer: Moving from bench to bed as next generation medicine. Oral Oncol. 2020 Dec; 111:104916. https://doi.org/10.1016/j.oraloncology.2020.104916 PMID: 32711289
9. Kent OA, Mendell JT. A small piece in the cancer puzzle: MicroRNAs as tumor suppressors and oncogenes. Oncogene. 2006 Oct; 25(46):6188–96. https://doi.org/10.1038/sj.onc.1209913 PMID: 17028598
10. Wu BH, Xiong XP, Jia J, Zhang WF. MicroRNAs: New actors in the oral cancer scene. Oral Oncol. 2011 May; 47(5):314–9. https://doi.org/10.1016/j.oraloncology.2011.03.019 PMID: 21474366
11. Yang Y, Li YX, Yang X, Jiang L, Zhou ZJ, Zhu YQ. Progress risk assessment of oral premalignant lesions with saliva miRNA analysis. BMC Cancer. 2013 Mar; 13:129. https://doi.org/10.1186/1471-2407-13-129 PMID: 23510112
12. Kozaki K, Imoto I, Mogi S, Omura K, Inazawa J. Exploration of tumor-suppressive microRNAs silenced by DNA hypermethylation in oral cancer. Cancer Res. 2008 Apr; 68(7):2094–105. https://doi.org/10.1158/0008-5472.CAN-07-5194 PMID: 18381414

13. Kunej T, Godnic I, Ferdin J, Horvat S, Dovc P, Calin GA. Epigenetic regulation of microRNAs in cancer: An integrated review of literature. Mutat Res. 2011 Dec; 717(1–2):77–84. https://doi.org/10.1016/j.mrfmmm.2011.03.008 PMID: 21420983

14. Gasche JA, Goel A. Epigenetic mechanisms in oral carcinogenesis. Future Oncol. 2012 Nov; 8 (11):1407–25. https://doi.org/10.2217/fon.12.138 PMID: 23148615

15. Santi DV, Garrett CE, Barr PJ. On the mechanism of inhibition of DNA-cytosine methyltransferases by cytosine analogs. Cell. 1983 May; 33(1):9–10. https://doi.org/10.1016/0092-8674(83)90327-6 PMID: 6205762

16. Venkatesh T, Nagashri MN, Swamy SS, Mohiyuddin SM, Gopinath KS, Kumar A. Primary microcephaly gene MCPH1 shows signatures of tumor suppressors and is regulated by miR-27a in oral squamous cell carcinoma. PLoS One. 2013; 8(3):e54643. https://doi.org/10.1371/journal.pone.0054643 PMID: 23472065

17. DBTSS University of Tokyo (Japan). https://dbtss.hgc.jp/.

18. Ladewig E, Okamura K, Flynt AS, Westholm JO, Lai EC. Discovery of hundreds of mirtrons in mouse and human small RNA data. Genome Res. 2012 Sep; 22(9):1634–45. https://doi.org/10.1101/gr.133553.111 PMID: 22955976

19. Navarro-Quiroz E, Pacheco-Lugo L, Navarro-Quiroz R, Lorenzi H, España-Puccini P, Díaz-Olmos Y, et al. Profiling analysis of circulating microRNA in peripheral blood of patients with class IV lupus nephritis. PLoS One. 2017 Nov; 12(11):e0187973. https://doi.org/10.1371/journal.pone.0187973 PMID: 29136041

20. Hiew MSY, Cheng HP, Huang CJ, Chong KY, Cheong SK, Choo KB, et al. Incomplete cellular reprogramming of colorectal cancer cells elicits an epithelial/mesenchymal hybrid phenotype. J Biomed Sci. 2018 Jul; 25(1):57. https://doi.org/10.1186/s12929-018-0461-1 PMID: 30025541

21. Otmani K, Lewalle P. Tumor suppressor miRNA in cancer cells and the tumor microenvironment: Mechanism of deregulation and clinical implications. Front Oncol. 2021 Oct; 11:708765. https://doi.org/10.3389/fonc.2021.708765 PMID: 34722255

22. More DA, Kumar A. SRSF3: Newly discovered functions and roles in human health and diseases. Eur J Cell Biol. 2020 Aug; 99(6):151099. https://doi.org/10.1016/j.ejcb.2020.151099 PMID: 32800280

23. Wang Z, Chatterjee D, Jeon HY, Akerman M, Vander Heiden MG, Cantley LC, et al. Exon-centric regulation of pyruvate kinase M alternative splicing via mutually exclusive exons. J Mol Cell Biol. 2012 Apr; 4(2):79–87. https://doi.org/10.1093/jmcb/mjr030 PMID: 22044881

24. Ajiro M, Jia R, Yang Y, Zhu J, Zheng ZM. A genome landscape of SRSF3-regulated splicing events and gene expression in human osteosarcoma U2OS cells. Nucleic Acids Res. 2016 Feb; 44(4):1854–70. https://doi.org/10.1093/nar/gkv1500 PMID: 26704980

25. Park SK, Jeong S. SRSF3 represses the expression of PDCD4 protein by coordinated regulation of alternative splicing, export and translation. Biochem Biophys Res Commun. 2016 Feb; 470(2):431–438. https://doi.org/10.1016/j.bbrc.2016.01.019 PMID: 26773498

26. Kim HR, Hwang SJ, Shin CH, Choi KH, Ohn T, Kim HH. SRSF3-regulated miR-132/212 controls cell migration and invasion by targeting YAP1. Exp Cell Res. 2017 Sep; 358(2):161–170. https://doi.org/10.1016/j.yexcr.2017.06.009 PMID: 28624413

27. Jia R, Li C, McCoy JP, Deng CX, Zheng ZM. SRp20 is a proto-oncogene critical for cell proliferation and tumor induction and maintenance. Int J Biol Sci. 2010 Dec; 6(7):806–26. https://doi.org/10.7150/ijbs.6.806 PMID: 21179588

28. He X, Arslan AD, Pool MD, Ho TT, Darcy KM, Coon JS, et al. Knockdown of splicing factor SRp20 causes apoptosis in ovarian cancer cells and its expression is associated with malignancy of epithelial ovarian cancer. Oncogene. 2011 Jan; 30(3):356–65. https://doi.org/10.1038/onc.2010.426 PMID: 20856201

29. Peiqi L, Zhaozhong G, Yaotian Y, Jun J, Jihua G, Rong J. Expression of SRSF3 is correlated with carcinogenesis and progression of oral squamous cell carcinoma. Int J Med Sci. 2016 Jun; 13(7):533–9. https://doi.org/10.7150/ijms.14871 PMID: 27429590

30. Guo J, Jia J, Jia R. PTBP1 and PTBP2 impaired autoregulation of SRSF3 in cancer cells. Sci Rep. 2015 Sep; 5:14548. https://doi.org/10.1038/srep14548 PMID: 26416554

31. Ghosh RD, Pattatheyil A, Roychoudhury S. Functional landscape of dysregulated microRNAs in oral squamous cell carcinoma: Clinical implications. Front Oncol. 2020 May; 10:619. https://doi.org/10.3389/fonc.2020.00619 PMID: 32547936

32. Mallela K, Shivananda S, Gopinath KS, Kumar A. Oncogenic role of miR-130a in oral squamous cell carcinoma. Sci Rep 2021. 11:7787. https://doi.org/10.1038/s41598-021-87388-4 PMID: 33833339

33. Rather MI, Nagashri MN, Swamy SS, Gopinath KS, Kumar A. Oncogenic microRNA-155 down-regulates tumor suppressor CDC73 and promotes oral squamous cell carcinoma cell proliferation:

Implications for cancer therapeutics. J Biol Chem. 2013 Jan; 288(1):608–18. https://doi.org/10.1074/jbc.M112.425736 PMID: 23166327

34. Wang JL, Guo CR, Sun TT, Su WY, Hu Q, Guo FF, et al. SRSF3 functions as an oncogene in colorectal cancer by regulating the expression of ArhGAP30. Cancer Cell Int. 2020 Apr; 20:120. https://doi.org/10.1186/s12935-020-01201-2 PMID: 32308565

35. Kurokawa K, Akaike Y, Masuda K, Kuwano Y, Nishida K, Yamagishi N, et al. Downregulation of serine/arginine-rich splicing factor 3 induces G1 cell cycle arrest and apoptosis in colon cancer cells. Oncogene. 2014 Mar; 33(11):1407–17. https://doi.org/10.1038/onc.2013.86 PMID: 23503458

36. Kim J, Park RY, Chen JK, Kim J, Jeong S, Ohn T. Splicing factor SRSF3 represses the translation of programmed cell death 4 mRNA by associating with the 5'-UTR region. Cell Death Differ. 2014 Mar; 21(3):481–90. https://doi.org/10.1038/cdd.2013.171 PMID: 24292556

37. Dhillon AS, Hagan S, Rath O, Kolch W. MAP kinase signalling pathways in cancer. Oncogene. 2007 May; 26(22):3279–90. https://doi.org/10.1038/sj.onc.1210421 PMID: 17496922

38. Chakraborty S, Mohiyuddin SM, Gopinath KS, Kumar A. Involvement of TSC genes and differential expression of other members of the mTOR signaling pathway in oral squamous cell carcinoma. BMC Cancer. 2008 Jun; 8:163. https://doi.org/10.1186/1471-2407-8-163 PMID: 18538015

39. Muranen T, Selfors LM, Worster DT, Iwanicki MP, Song L, Morales FC, et al. Inhibition of PI3K/mTOR leads to adaptive resistance in matrix-attached cancer cells. Cancer Cell. 2012 Feb; 21(2):227–39. https://doi.org/10.1016/j.ccr.2011.12.024 PMID: 22340595

40. Baskerville S, Bartel DP. Microarray profiling of microRNAs reveals frequent coexpression with neighboring miRNAs and host genes. RNA. 2005 Mar; 11(3):241–7. https://doi.org/10.1261/rna.7240905 PMID: 15701730

41. Lin SL, Miller JD, Ying SY. Intronic microRNA (miRNA). J Biomed Biotechnol. 2006; 2006(4):26818. https://doi.org/10.1155/JBB/2006/26818 PMID: 17057362

42. Monteys AM, Spengler RM, Wan J, Tecedor L, Lennox KA, Xing Y, et al. Structure and activity of putative intronic miRNA promoters. RNA. 2010 Mar; 16(3):495–505. https://doi.org/10.1261/rna.1731910 PMID: 20075166

43. White JS, Weissfeld JL, Ragin CC, Rossie KM, Martin CL, Shuster M, et al. The influence of clinical and demographic risk factors on the establishment of head and neck squamous cell carcinoma cell lines. Oral Oncol. 2007 Aug; 43(7):701–12. https://doi.org/10.1016/j.oraloncology.2006.09.001 PMID: 17112776

44. Chen Y, Wang X. miRDB: an online database for prediction of functional microRNA targets. Nucleic Acids Res. 2020 Jan 8; 48(D1):D127–D131 https://doi.org/10.1093/nar/gkz757 PMID: 31504780

45. Paraskevopoulou MD, Georgakilas G, Kostoulas N, Vlachos IS, Vergoulis T, Reczko M, et al. DIANA-microT web server v5.0: service integration into miRNA functional analysis workflows. Nucleic Acids Res. 2013 Jul; 41(Web Server issue):W169–73. https://doi.org/10.1093/nar/gkt393 PMID: 23680784

46. Reczko M, Maragkakis M, Alexiou P, Grosse I, Hatzigeorgiou AG. Functional microRNA targets in protein coding sequences. Bioinformatics. 2012 Mar 15; 28(6):771–6. https://doi.org/10.1093/bioinformatics/bts043 PMID: 22285563

47. McGeary SE, Lin KS, Shi CY, Pham TM, Bisaria N, Kelley GM, et al. The biochemical basis of microRNA targeting efficacy. Science. 2019 Dec 20; 366(6472):eaav1741. https://doi.org/10.1126/science.aav1741 PMID: 31806698

48. Sobin LH, Fleming ID. TNM Classification of Malignant Tumors, fifth edition (1997). Union Internationale Contre le Cancer and the American Joint Committee on Cancer. Cancer. 1997 Nov; 80(9):1803–4. https://doi.org/10.1002/(sici)1097-0142(19971101)80:9<1803::aid-cncr16>3.0.co;2-9 PMID: 9351551

49. Sharbati-Tehrani S, Kutz-Lohroff B, Bergbauer R, Scholven J, Einspanier R. miR-Q: A novel quantitative RT-PCR approach for the expression profiling of small RNA molecules such as miRNAs in a complex sample. BMC Mol Biol. 2008 Apr; 9:34. https://doi.org/10.1186/1471-2199-9-34 PMID: 18400113

50. Sambrook J, Maniatis RH, Fristsch EF. Molecular cloning: a laboratory manual. New York: ColdSpring Harbor Laboratory Press. 1995.

51. Pradhan SA, Rather MI, Tiwari A, Bhat VK, Kumar A. Evidence that TSC2 acts as a transcription factor and binds to and represses the promoter of Epiregulin. Nucleic Acids Res. 2014 Jun; 42(10):6243–55. https://doi.org/10.1093/nar/gku278 PMID: 24748662

52. Karimi L, Zeinali T, Hosseinahli N, Mansoori B, Mohammadi A, Yousefi M, et al. miRNA-143 replacement therapy harnesses the proliferation and migration of colorectal cancer cells in vitro. J Cell Phys. 2019; 234(11):21359–21368. https://doi.org/10.1002/jcp.28745 PMID: 31032951

53. Horibata S, Vo TV, Subramanian V, Thompson PR, Coonrod SA. Utilization of the soft agar colony formation assay to identify inhibitors of tumorigenicity in breast cancer cells. J Vis Exp. 2015 May; (99): e52727. https://doi.org/10.3791/52727 PMID: 26067809